




G α -13 induces CXC motif chemokine ligand 5 expression in prostate cancer cells by transactivating NF- κ B

Received for publication, July 1, 2019, and in revised form, October 3, 2019. Published, Papers in Press, October 21, 2019, DOI 10.1074/jbc.RA119.010018

Wei Kiang Lim[‡], Xiaoran Chai[§], Sujoy Ghosh[§], Debleena Ray[‡], Mei Wang[‡],  Suhail Ahmed Kabeer Rasheed^{‡1}, and Patrick J. Casey^{‡1,2}

From the [‡]Programme in Cancer and Stem Cell Biology and [§]Programme in Cardiovascular and Metabolic Disorders, Duke-NUS Medical School, 169857 Singapore and the ¹Department of Pharmacology and Cancer Biology, Duke University Medical Center, Durham, North Carolina 27710

Edited by Henrik G. Dohlman

GNA13, the α subunit of a heterotrimeric G protein, mediates signaling through G-protein-coupled receptors (GPCRs). GNA13 is up-regulated in many solid tumors, including prostate cancer, where it contributes to tumor initiation, drug resistance, and metastasis. To better understand how GNA13 contributes to tumorigenesis and tumor progression, we compared the entire transcriptome of PC3 prostate cancer cells with those cells in which GNA13 expression had been silenced. This analysis revealed that GNA13 levels affected multiple CXC-family chemokines. Further investigation in three different prostate cancer cell lines singled out pro-tumorigenic CXC motif chemokine ligand 5 (CXCL5) as a target of GNA13 signaling. Elevation of GNA13 levels consistently induced CXCL5 RNA and protein expression in all three cell lines. Analysis of the CXCL5 promoter revealed that the $-505/+62$ region was both highly active and influenced by GNA13, and a single NF- κ B site within this region of the promoter was critical for GNA13-dependent promoter activity. ChIP experiments revealed that, upon induction of GNA13 expression, occupancy at the CXCL5 promoter was significantly enriched for the p65 component of NF- κ B. GNA13 knockdown suppressed both p65 phosphorylation and the activity of a specific NF- κ B reporter, and p65 silencing impaired the GNA13-enhanced expression of CXCL5. Finally, blockade of Rho GTPase activity eliminated the impact of GNA13 on NF- κ B transcriptional activity and CXCL5 expression. Together, these findings suggest that GNA13 drives CXCL5 expression by transactivating NF- κ B in a Rho-dependent manner in prostate cancer cells.

Prostate cancer is the second most prevalent cancer in males and is currently ranked the 5th leading cause of cancer deaths worldwide (1). The major reasons for death from prostate can-

cer are metastasis, drug resistance, and tumor relapse (2). As such, identifying the cellular mechanisms that contribute to prostate tumorigenesis and cancer progression would aid in the development of novel therapeutics to improve outcomes (3). Although previous studies on prostate cancer signaling have mostly focused on androgen hormone-signaling pathways, recent investigations have implicated G-protein-coupled receptors (GPCRs)³ and their downstream signaling molecules in prostate cancer initiation and progression (3, 4).

GPCRs are the largest and most diverse group of integral membrane proteins in eukaryotes. These proteins mediate cellular responses to a wide variety of ligands and are also important for numerous physiological functions (5). GPCRs are coupled to heterotrimeric G proteins that are made up of G α , G β , and G γ subunits, from which the G α class can be further categorized into the G s , G q , G i , and G 12 subfamilies (6). Heterotrimeric G proteins function as molecular switches; ligand binding to the GPCR triggers a conformational change in the transmembrane region of the receptor, resulting in a GDP-GTP exchange on the G α subunit and its subsequent dissociation from the G $\beta\gamma$ dimer (6, 7). The G α protein then interacts with its specific downstream effectors to regulate different signaling pathways (6–8). Recently, several ligand/GPCR pairs, including SDF-1/CXCR4, lysophosphatidic acid/LPAR, thrombin/PAR1, and sphingosine 1-phosphate/S1PR, have been reported to be involved in cancer cell invasion, metastasis, and drug resistance, ultimately leading to poor prognosis of the cancers (4). Interestingly, most of these GPCRs signal through the G 12 subfamily of heterotrimeric G proteins (8).

The G 12 subfamily of G proteins consists of the GNA12 and GNA13 proteins (8). Both 43-kDa proteins, GNA12 and GNA13 are expressed in many tissues and are involved in mul-

This work was supported by National Medical Research Council Grants NMRC/BNIG/2041/2015 (to S. A. K. R.) and NMRC/CBRG/0044/2013 (to P. J. C.) and Ministry of Education Grant MOE2018-T2-1-147 (to P. J. C.). The authors declare that they have no conflicts of interest with the contents of this article.

This article contains Figs. S1–S5 and Tables S1–S5.

¹ To whom correspondence may be addressed: Program in Cancer and Stem Cell Biology, Duke-NUS Medical School, 8 College Rd., 169857 Singapore. Tel.: 65-66013741; E-mail: kabeer.rasheed@duke-nus.edu.sg.

² To whom correspondence may be addressed: Program in Cancer and Stem Cell Biology, Duke-NUS Medical School, 8 College Rd., 169857 Singapore. Tel.: 65-65167251; E-mail: patrick.casey@duke-nus.edu.sg.

³ The abbreviations used are: GPCR, G-protein-coupled receptor; GNA13, G-protein subunit α -13; GNA12, G-protein subunit α -12; CXCL1, CXC motif chemokine ligand 1; CXCL2, CXC motif chemokine ligand 2; CXCL3, CXC motif chemokine ligand 3; CXCL4, CXC motif chemokine ligand 4; CXCL5, CXC motif chemokine ligand 5; CXCL6, CXC motif chemokine ligand 6; CXCL7, CXC motif chemokine ligand 7; CXCL8, CXC motif chemokine ligand 8; NF- κ B, nuclear factor κ B; P65/RelA, RelA proto-oncogene, NF- κ B subunit; SDF-1, stromal cell-derived factor 1; CXCR4, CXC motif chemokine receptor 4; LPAR, lysophosphatidic acid receptor; PAR1, protease-activated receptor 1; S1PR, sphingosine 1-phosphate receptor; RhoA, Ras homolog family member A; ROCK, Rho-associated protein kinase; HPRT, hypoxanthine-guanine phosphoribosyltransferase; FBS, fetal bovine serum; RLU, relative light unit; PMSF, phenylmethylsulfonyl fluoride.

multiple physiological and developmental processes (10). In terms of cancer biology, both these proteins have been shown to be up-regulated in breast, head and neck, gastric, and prostate cancers (11–15). Previous work by our laboratory reported that blocking GNA12/13 signaling leads to significant suppression of cancer cell invasion *in vitro* and metastasis *in vivo* in breast and prostate cancers (11, 12). In our recent studies, we demonstrated that blocking GNA13 alone significantly impacts cancer cell invasion and metastasis in prostate and breast cancers (16, 17). Furthermore, in head and neck cancers, GNA13, but not GNA12, was found to be a biomarker for drug resistance and poor prognosis. In the same study, GNA13 was also reported to induce tumor initiating or cancer stem cell-like phenotypes (13). Although these studies from our group and others have indicated the importance of GNA13 in tumor growth and progression, the mechanisms that mediate GNA13-induced oncogenesis are not well-understood.

In this study, we performed analysis of global gene expression changes in a highly-metastatic prostate cancer (PC3) cell line. The analysis identified a set of chemokines that belong to the CXC-chemokine family to be significantly down-regulated upon knockdown of GNA13 in PC3 cells. Subsequent validation studies in three different prostate cancer cells identified CXCL5 as a direct target of GNA13 signaling in prostate cancer cells. Interestingly, CXCL5 has recently been implicated in tumor growth, drug resistance, and metastasis in many different solid tumors, including prostate cancers (18–21). Through a series of studies, we show that GNA13 controls CXCL5 expression through the transactivation of the NF- κ B–signaling pathway in a fashion that depends on Rho GTPases. Identifying GNA13 as a regulator of CXCL5 expression should aid in better understanding of this G protein and its effect on biological processes that promote cancer progression.

Results

GNA13 induces CXC-chemokines in PC3 cells

Previously, we showed that GNA13 expression correlates with the aggressiveness of prostate cancer cells and that blocking GNA13 expression or activity inhibits cancer cell invasion and metastasis (16). However, the mechanism(s) that mediate GNA13-induced cancer cell invasion and metastasis in prostate cancer cells are not well-understood. To address this issue, gene expression analysis was performed in the PC3 cell line. PC3 cells express high basal levels of GNA13, and hence a comparison was made of gene expression profiles of the control line and that in which GNA13 expression was silenced. Both GNA13 protein and RNA levels were significantly reduced in PC3 cells that express two different sh-RNAs targeting GNA13 (sh-GNA13-1, and -2) as compared with the control cells (Fig. 1A). Total RNA was extracted from these cell lines and subjected to RNA-Seq and Ingenuity Pathway Analysis (IPA) analysis of the data (Fig. 1B). A cutoff for gene expression changes of a log₂ fold-change of -1 or $+1$ against sh-RNA control cells, together with a p value of 0.05, was used to shortlist genes that were down- or up-regulated in both sh-GNA13-1 and -2 (Fig. 1B). Ultimately, 54 genes were found to be up-regulated, whereas 102 genes were down-regulated with GNA13 knock-

down using both sh-RNAs (Fig. 1B). Interestingly, CXC-family chemokines, CXCL1–3, -5, -6, and -8, were among the genes that were significantly down-regulated (p value <0.001) upon suppression of GNA13 in cells expressing either sh-RNA-1 or -2 (Fig. 1C). Moreover, analysis by IPA predicted that these chemokines are involved in the metastasis of cells (Fig. 1D). As it has been previously reported that GNA13 is up-regulated in solid tumors and impacts patient survival and metastasis (13, 16, 17), these chemokines were selected as targets for further validation.

GNA13 drives CXCL5 expression in multiple prostate cancer cells

A preliminary screen of RNA expression of CXC-chemokines 1–8 (CXCL1–8) by real-time PCR showed that, consistent with RNA-Seq data, most CXCL-mRNAs were down-regulated when GNA13 expression was suppressed in PC3 cells (Fig. 2A). To filter through these targets, another prostate cancer cell line that expresses moderately high levels of GNA13 under normal conditions, *i.e.* Du145, was employed. GNA13 was efficiently knocked down in these cells with the same set of sh-RNAs as in PC3 cells (Fig. 2B). In Du145 cells, however, most chemokines tested showed marginal changes in mRNA levels upon silencing of GNA13 expression, with the notable exception of CXCL5 (Fig. 2B). To validate the finding that CXCL5 expression in prostate cancer cells was highly dependent on GNA13, we determined mRNA levels of the same set of CXC-chemokines in LnCaP cells, a poorly-aggressive prostate cancer cell line that expresses relatively low levels of GNA13. Analysis of CXC-chemokine expression in control LnCaP cells (pBabe-vector) *versus* those with enforced expression of GNA13 (pBabe-GNA13) revealed that CXCL5 expression was highly dependent on GNA13 levels in this cell line (Fig. 2C).

Because the CXCL5 gene encodes for a secreted protein, we next assessed the impact of GNA13 levels on the production of the actual chemokine. To this end, CXCL5 protein present in cell culture media was quantitatively measured using ELISA. Upon suppression of GNA13 expression in both PC3 and Du145 cells, the levels of secreted CXCL5 were substantially decreased as compared with the control cells (Fig. 2D). Conversely, the enforced expression of GNA13 in LnCaP cells resulted in markedly increased CXCL5 protein in the media (Fig. 2D). These results show that both CXCL5 RNA and protein expression correspond to GNA13 levels in prostate cancer cells. To further substantiate the link between GNA13 levels and CXCL5 expression, a doxycycline-inducible GNA13 expression construct was employed in the PC3 knockdown cells. When GNA13 was re-introduced into the GNA13 knockdown cells (sh-GNA13) exogenously, CXCL5 mRNA expression and the levels of secreted chemokine were restored to levels similar to that of the WT cells (sh-RNA–Control) within 72–96 h of doxycycline induction (Fig. 2E). Most importantly, analysis of GNA13 and CXCL5 in TCGA datasets showed that a significant correlation exists between GNA13 and CXCL5 RNA expression in prostate tumor samples, providing additional support for an association between GNA13 and CXCL5 in human prostate cancers (Spearman correlation, $R = 0.4$, p value <0.0001 ; Fig. 2F). Taken together, these findings indicate

GNA13 induces CXCL5 expression in prostate cancers

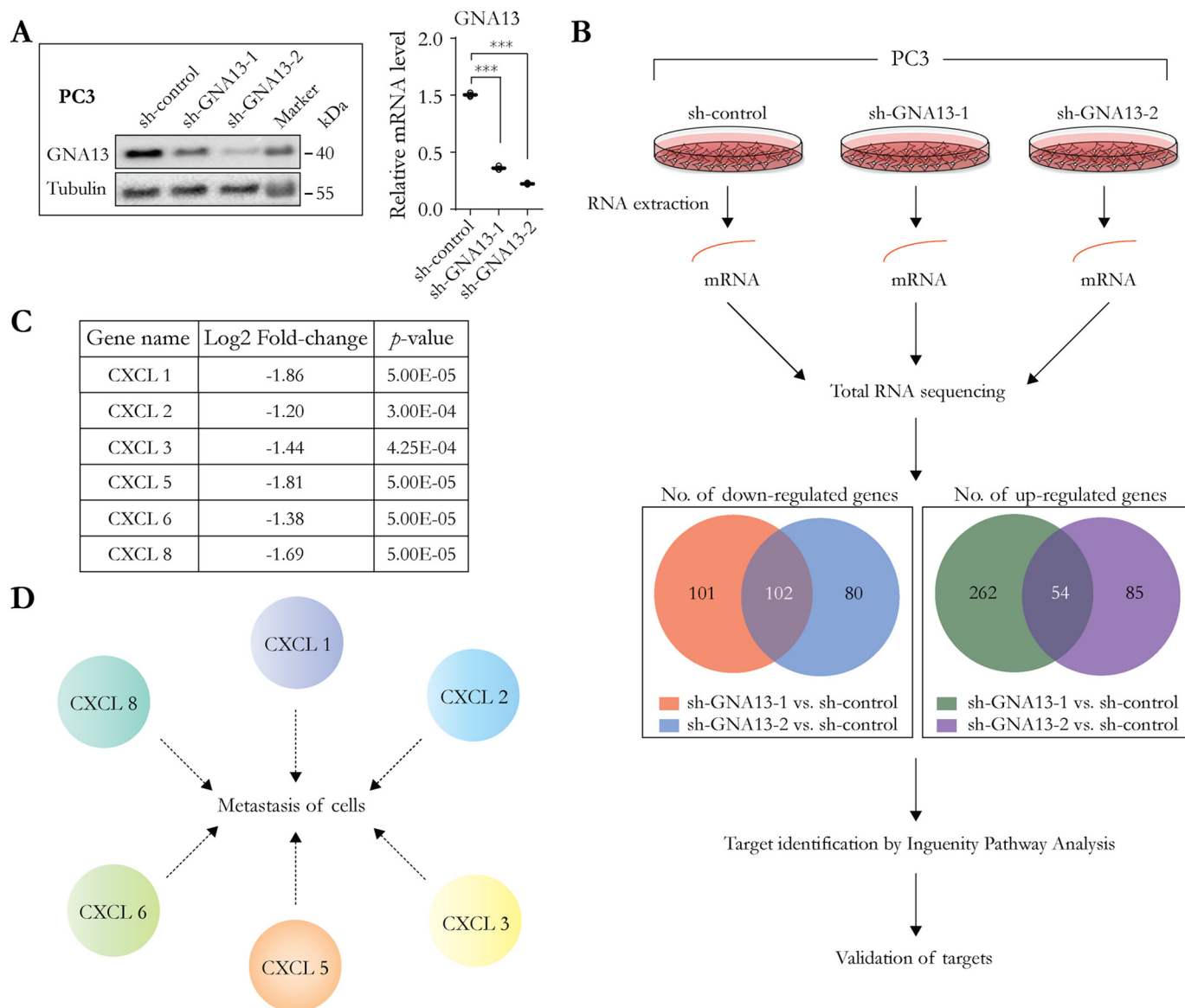


Figure 1. Silencing of GNA13 impacts expression of CXC-chemokines in PC3 cells. *A*, GNA13 protein and RNA levels in PC3 cells stably expressing two different sh-RNAs (sh-GNA13-1 and -2) targeting GNA13 compared with sh-RNA-control (indicated as *sh-control*) cells. *Immunoblot* shows GNA13 protein levels, probed using a GNA13-specific antibody. Tubulin was included as a loading control. mRNA expression of GNA13 is shown relative to that of HPRT, which was used as a normalizing control. Data are presented as mean \pm S.D., and *p* values are denoted as ***, $p < 0.001$. *B*, schematic of experimental workflow for the identification of genes that are regulated by GNA13 in PC3 cells. The *Venn diagram* within shows the number of genes that were down- or up-regulated upon suppression of GNA13 expression in PC3 sh-GNA13-1 and sh-GNA13-2 cells as compared with sh-control cells. Genes that showed a log₂ fold-change of +1 or greater was considered up-regulated, and a fold-change of -1 or greater was considered as down-regulated, with a minimum *p* value of 0.05. *C*, list of differentially-expressed CXC-chemokines in PC3 cells expressing sh-RNAs targeting GNA13 compared with cells expressing sh-control alone. Shown are the fold-change and statistical significance of CXC-chemokine genes identified from total RNA-Seq to be down-regulated upon GNA13 knockdown (values indicated are averages of sh-GNA13-1 and sh-GNA13-2), as compared with sh-control cells. *D*, schematic showing predicted pathway involvement of selected CXC-chemokines, as determined using ingenuity pathway analysis.

that CXCL5 expression in prostate cancer cells is substantially influenced by GNA13 levels.

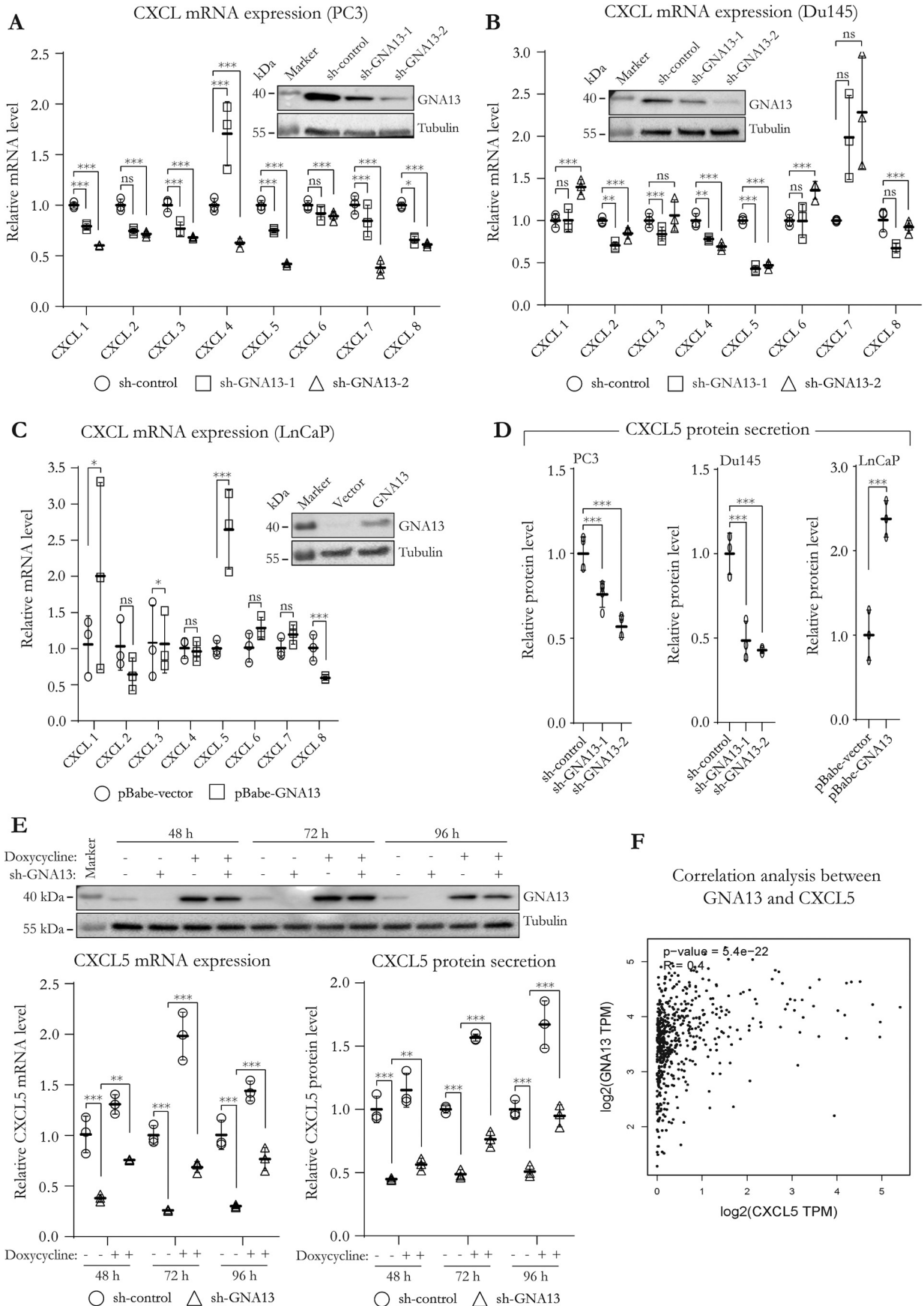
GNA12 does not impact CXCL5 expression

To test whether GNA12, the other G12 family member that is 67% identical to GNA13 by sequence, influences CXCL5 expression, two sh-RNAs targeting GNA12 (sh-GNA12-1 and -2) were used to knock down the protein in PC3 cells (where GNA12 is also highly expressed), and CXCL5 RNA expression was measured. Interestingly, the suppression of GNA12 expression in PC3 cells had no impact on CXCL5 expression (Fig. 3A).

Similarly, the enforced expression of GNA12 in LnCaP cells (which contain very low levels of the GNA12 protein) had no impact on CXCL5 mRNA expression (Fig. 3A). These data clearly show that it is the levels of GNA13, and not GNA12, that impact CXCL5 expression in prostate cancer cells.

GNA13-induced CXCL5 expression depends on NF- κ B activation

The data presented so far suggest that the impact of GNA13 on CXCL5 expression is at the transcriptional level. To assess this impact of GNA13, luciferase reporter constructs driven by



GNA13 induces CXCL5 expression in prostate cancers

a CXCL5 promoter fragment containing -2324 (upstream) to $+62$ (downstream) bases relative to the transcription start site and 500-bp serial truncations of the full promoter were cloned into the pGL3-Basic-Luciferase reporter system (Fig. 3B). Equal amounts of either pGL3-CXCL5-Luc or the promoter-less pGL3-basic vector were transfected into two prostate cancer cells expressing high levels of GNA13, *i.e.* PC3 and Du145. Truncations in the promoter led to stepwise increases in CXCL5-luciferase expression in both the PC3 and Du145 cells (Fig. 3C), with the $-505/+62$ region of the CXCL5-promoter construct exhibiting the highest activity. Furthermore, deletion of the $-505/+62$ region of the CXCL5 promoter completely abrogated reporter activity, indicating that this region is not only highly active but is also the minimally required promoter region for CXCL5 expression in prostate cancer cells (Fig. 3C). Most importantly, knockdown of GNA13 in both PC3 (Fig. 3D) and Du145 (Fig. 3E) cells suppressed luciferase reporter activity of the CXCL5-promoter constructs, with the strongest impact seen with the $-505/+62$ element. In confirmation of this promoter region being the most important for the impact of GNA13, an opposite effect was seen on reporter activity in LnCaP cells upon enforced expression of GNA13 (Fig. 3F). These data strongly suggest that crucial transcriptional element(s) of the CXCL5 promoter that respond to GNA13 bind within the $-505/+62$ region of the promoter.

In the first step to identify regulatory molecules that interact with the CXCL5 promoter, the $-505/+62$ promoter sequence was analyzed using two independent transcription factor-binding prediction tools (Alibaba2.1 and MatrixCatch) to identify possible binding sites. Both tools identified an NF- κ B-binding site with sequence GGGAATTTC at position -29 to -38 bp upstream of the transcriptional start site (Fig. 4A). As GNA13 has previously been implicated in NF- κ B signaling in a different cell type (22), the potential involvement of NF- κ B on GNA13-driven CXCL5 expression in prostate cancer cells was investigated. The NF- κ B-binding site was removed by either truncation or by employing a five-nucleotide deletion (AATTT) of the site from -31 to -35 bp (Fig. 4A). Assessment of luciferase expression using these constructs showed that such disruption of the NF- κ B-binding site in the CXCL5 promoter almost completely abrogated CXCL5 promoter-driven luciferase signals in PC3 and Du145, and further knockdown of GNA13 had no additional impact on promoter activity (Fig. 4, B and C).

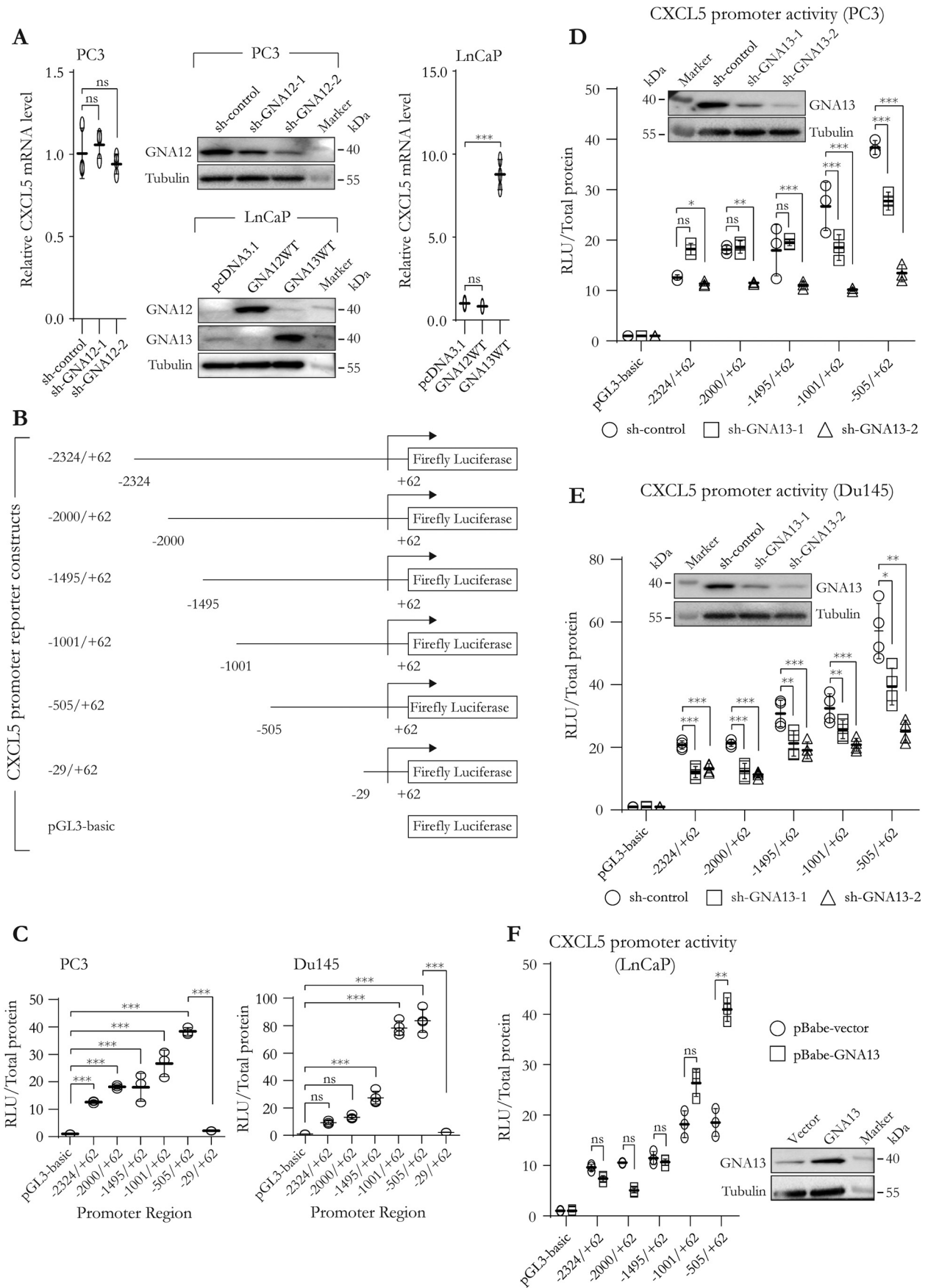
Further evidence of the importance of the $-505/+62$ CXCL5 promoter region came from the use of the LnCaP GNA13 over-expression model, where GNA13-dependent activity of the promoter construct was suppressed when the NF- κ B-binding site was disrupted (Fig. 4D).

To confirm the association of the NF- κ B transcription factor with the CXCL5 promoter, and the impact of GNA13 levels on this association, ChIP was performed in LnCaP control cells and those with enforced expression of GNA13. Real-time PCR analysis of p65-bound DNA (a major component of NF- κ B transcriptional complex) showed a significant enrichment of p65 binding to the predicted NF- κ B site on the CXCL5 promoter upon enforced expression of GNA13 in LnCaP cells when compared with the vector control (Fig. 4E). Analysis of I κ B α promoter as a positive control for NF- κ B (p65) binding to the chromatin showed similar results (Fig. 4E). Taken together, these findings indicate that the impact of GNA13 on CXCL5 expression is mediated through NF- κ B binding to the CXCL5 promoter. More importantly, these data show that GNA13 is a key driver of NF- κ B transcriptional activity in prostate cancer cells.

GNA13 induces NF- κ B-signaling pathway

The data so far indicate that GNA13 drives transcription of CXCL5 by inducing the transactivation of NF- κ B in prostate cancer cells. Consistent with this assessment, gene set enrichment analysis of all the genes identified through RNA-Seq to be down-regulated upon GNA13 silencing in PC3 cells revealed that GNA13 broadly impacts the NF- κ B transcriptional program in prostate cancer cells (Table S1). To obtain direct evidence for GNA13 modulation of NF- κ B signaling in prostate cancer cells, phosphorylation of the p65 subunit of the NF- κ B complex was assessed. Phosphorylation of p65 is one of the key initial steps in the activation of the NF- κ B-signaling pathway. In starved parental PC3 (Fig. 5A) and Du145 (Fig. 5B) cells, serum stimulation induced the phosphorylation of p65 substantially. However, this phosphorylation was suppressed upon knockdown of GNA13 in both these cells (Fig. 5, A and B). Consistent with this observation, p65 phosphorylation was enhanced in LnCaP cells upon enforced expression of GNA13 when compared with control cells (Fig. 5C). To further probe the capacity of GNA13 in regulating the transcriptional function of NF- κ B, a promoter-reporter construct driven solely by

Figure 2. GNA13 drives CXCL5 expression in prostate cancer cells. CXCL-chemokines' mRNA levels in PC3 (A) and Du145 (B) cells. Shown is the impact of GNA13 knockdown on RNA levels of various CXC family chemokines (CXCL1–8) that were short-listed from total RNA-Seq and ingenuity pathway analysis of the experiment described in Fig. 1. RNA levels were assessed by real-time PCR; relative mRNA expression was plotted as fold-change to control cells (*sh-GNA13-1* or *sh-GNA13-2* compared with *sh-control*). HPRT was used as a normalizing control. The immunoblots show the knockdown efficiency of GNA13 in PC3 (A) and Du145 (B) cells. C, ectopic expression of GNA13 enhances CXCL5 expression in LnCaP cells. Shown are the RNA levels of the indicated CXC-chemokines following enforced expression of GNA13 in LnCaP cells compared with that of vector-expressing control cells (pBabe-GNA13 versus pBabe-vector). GNA13 protein levels in LnCaP cells stably expressing either pBabe-vector or p-Babe-GNA13 are shown in the immunoblot; tubulin was also probed as a loading control. D, GNA13 levels impact CXCL5 protein secretion in three different prostate cancer cells. Shown are the relative levels of secreted CXCL5 protein in conditioned media collected 48 h after GNA13 knockdown (PC3, Du145) or overexpression (LnCaP). Relative CXCL5 protein levels are plotted as fold-change compared with control cells in each case. CXCL5 levels were quantified using an ELISA (see under "Experimental procedures"). E, enforced expression of GNA13 rescues CXCL5 expression in PC3 cells in which GNA13 had been silenced. Shown is the effect of exogenously restoring GNA13 levels on CXCL5 mRNA and protein levels across the three indicated time points of induction of GNA13 with 10 ng/ml doxycycline in a tetracycline-inducible system. mRNA or protein expression is plotted as fold-change relative to the untreated control set at each time point. F, CXCL5 expression correlates with GNA13 levels in human samples. The positive relationship between GNA13 and CXCL5 RNA expression in human normal and tumor prostate samples is shown. Log2 expression of CXCL5 mRNA is plotted versus GNA13 mRNA expression in transcripts per kb million. Correlation analysis was performed using GEPIA analysis tool and Spearman rank correlation. (p value = 5.4×10^{-22} , $R = 0.4$ (Spearman correlation)). p values are calculated from three independent experiments; results shown are a representative of those three. Plotted data are presented as mean \pm S.D., and p values are denoted as follows: *, $p < 0.05$; **, $p < 0.01$; and ***, $p < 0.001$ or ns for not significant.



GNA13 induces CXCL5 expression in prostate cancers

NF- κ B, which consists of six repeats of the NF- κ B consensus sequence driving luciferase expression (6X-NF- κ B-luciferase), was employed. Assessment of luciferase activity of this construct under conditions of differential GNA13 expression revealed that knockdown of GNA13 significantly reduced 6X-NF- κ B reporter activity in both PC3 and Du145 cells (Fig. 5D). On the flipside, enforced expression of GNA13 significantly enhanced 6X-NF- κ B-driven firefly luciferase expression in LnCaP cells (Fig. 5D).

The evidence presented so far indicates that GNA13-induced expression of CXCL5 is mediated via NF- κ B activation in prostate cancer cells. To further test this hypothesis, we silenced p65 (also termed as RelA) expression in LnCaP control cells and those with enforced expression of GNA13 using two different si-RNAs (denoted as si-RelA and si-RelA-1 or si-RelA-2) directed against p65. Silencing of p65 expression by either si-RNAs led to a substantial (50–60%) reduction in GNA13-induced CXCL5 mRNA expression (Fig. 6A). However, in the PC3 and Du145 cell models, si-RNA-directed silencing of p65 suppressed CXCL5 mRNA expression in the WT (sh-RNA-control) cells, although no effect was observed in cells that express the sh-RNAs against GNA13 (Fig. S1). These observations clearly show that silencing NF- κ B protein expression significantly impairs GNA13-induced CXCL5 transcription in prostate cancer cells. Taken together, these data indicate that GNA13 is an important upstream mediator of the NF- κ B-signaling pathway in prostate cancer cells, and the impact of GNA13 on NF- κ B signaling plays a crucial role in the induction of CXCL5 expression in these cells.

GNA13 regulation of CXCL5 expression by NF- κ B depends on Rho GTPase function

Rho GTPases are the best-characterized downstream effectors of GNA12/GNA13 signaling (23, 24). Consistent with these previous studies, enforced GNA13 expression led to enhanced RhoA activation in LnCaP cells (Fig. 6B). To test whether this GNA13-mediated activation of RhoA is important for CXCL5 expression, the cells were treated with C3 toxin, a well-characterized inhibitor of Rho family GTPases that induces ADP-ribosylation of its targets (25–27). As expected, the presence of C3 toxin led to reduced GTP-bound RhoA (active RhoA), along with a reduction in total RhoA protein levels (Fig. 6B), in LnCaP vector or GNA13-expressing cells. Most importantly, measurement of CXCL5 levels by real-time

PCR following treatment with C3 toxin revealed that the GNA13-induced CXCL5 expression was severely impacted when Rho proteins were inactivated by C3 toxin (Fig. 6B), suggesting a GNA13-dependent involvement of Rho GTPases in the regulation of CXCL5 expression. This observation was also made with the Du145 cells, where GTP-bound Rho (active Rho) was greatly enhanced upon addition of FBS in a WT setting, but this Rho activation was significantly repressed upon GNA13 knockdown (Fig. S2). These data indicate that GNA13 mediates the activation of Rho proteins and that inhibition of Rho activity significantly suppresses GNA13-induced CXCL5 mRNA expression in prostate cancer cells.

We also assessed the impact of treatment with C3 toxin on the GNA13-induced reporter activity of the $-505/+62$ -CXCL5 promoter and the 6X-NF- κ B reporter (Fig. 6C). Expression of C3 toxin in LnCaP cells markedly suppressed the GNA13-induced activity of both the CXCL5 promoter- and 6X-NF- κ B-luciferase reporter activities (Fig. 6C). To further confirm the involvement of Rho GTPases in GNA13-dependent CXCL5 expression, a dominant-negative mutant form of RhoA, which interferes with the activation of multiple Rho GTPase family members (28, 29), was employed. Consistent with the C3 toxin inactivation data, GNA13-induced CXCL5 mRNA expression was significantly suppressed upon overexpression of the dominant-negative RhoA (Fig. 6D). Taken together, these findings show that GNA13 signals through Rho proteins to induce the transactivation of NF- κ B and consequently control expression of CXCL5.

Discussion

Despite significant progress made in diagnosis and treatment, prostate cancer mortality has not improved significantly over the years, largely due to drug resistance and metastasis of the cancer (3). Identifying novel mechanisms that drive resistance to therapy and metastasis could help us develop novel combination therapies to improve therapeutic outcomes. The G_{12} family of G proteins, which includes both GNA12 and GNA13, and the GPCRs associated with them have been widely implicated in cancer progression (6, 8, 30). In prostate cancers, GNA13 levels correlate with aggressiveness, and blocking GNA13 alone could significantly impact cancer cell invasion toward SDF-1 (16). In addition, we and others have shown that GNA13 is a biomarker for poor prognosis and an inducer of multidrug resistance and metastasis in solid tumors (13, 15).

Figure 3. GNA13 induces CXCL5 expression in an NF- κ B-dependent manner in prostate cancer cells. A, GNA12 levels do not impact CXCL5 expression in prostate cancer cells. The left panel shows CXCL5 RNA levels in PC3 cells stably expressing two different sh-RNAs against GNA12 (*sh-GNA12-1* and *sh-GNA12-2*) or vector control (*control*), plotted as fold-change relative to the control cells. GNA12 protein level in these cells is shown in the upper middle panel. The lower middle panel shows immunoblot analysis of GNA12 and GNA13 protein expression in LnCaP cells transiently transfected with GNA12- or GNA13-expressing plasmids, or pCDNA3.1 vector, for 48 h. The right panel shows the impact of enforced expression of GNA12 or GNA13 on CXCL5 RNA levels, as compared with the vector control in both cases (*GNA12WT versus pCDNA3.1* or *GNA13WT versus pCDNA3.1*, respectively). B, schematic diagram of the construction of CXCL5 promoter-derived luciferase reporter constructs. The CXCL5 promoter containing bp -2324 to $+62$ relative to the transcriptional start site and the serial truncations therefrom were cloned into pGL3-basic as detailed under "Experimental procedures." C, luciferase reporter activity driven by the indicated CXCL5 promoter constructs in PC3 (left panel) and Du145 (right panel) cells. D and E, graphs show the impact of suppressing GNA13 expression in PC3 (D) and Du145 (E) cells on CXCL5 promoter activity. Shown is the promoter activity driven by the indicated CXCL5 promoter constructs in parental cells (sh-RNA-control) and those in which GNA13 was knocked down using sh-RNA-1 or sh-RNA-2 as indicated. F, impact of enforced expression of GNA13 on the activity of CXCL5 promoter elements in control LnCaP cells (expressing pBabe-vector) compared with those with enforced expression of GNA13 (pBabe-GNA13). All reporter data are plotted as the ratio of relative light units (RLU) of reporter to total protein, plotted as fold-change relative to the pGL3-basic vector in each of the respective control cells. GNA13 expression is shown in immunoblots in D–F for each of the cell lines, respectively. *p* values are calculated from three independent experiments; the results shown are a representative of those three. Plotted data are presented as mean \pm S.D., and *p* values are denoted as follows: *, *p* < 0.05; **, *p* < 0.01; and ***, *p* < 0.001 or *ns* for not significant.

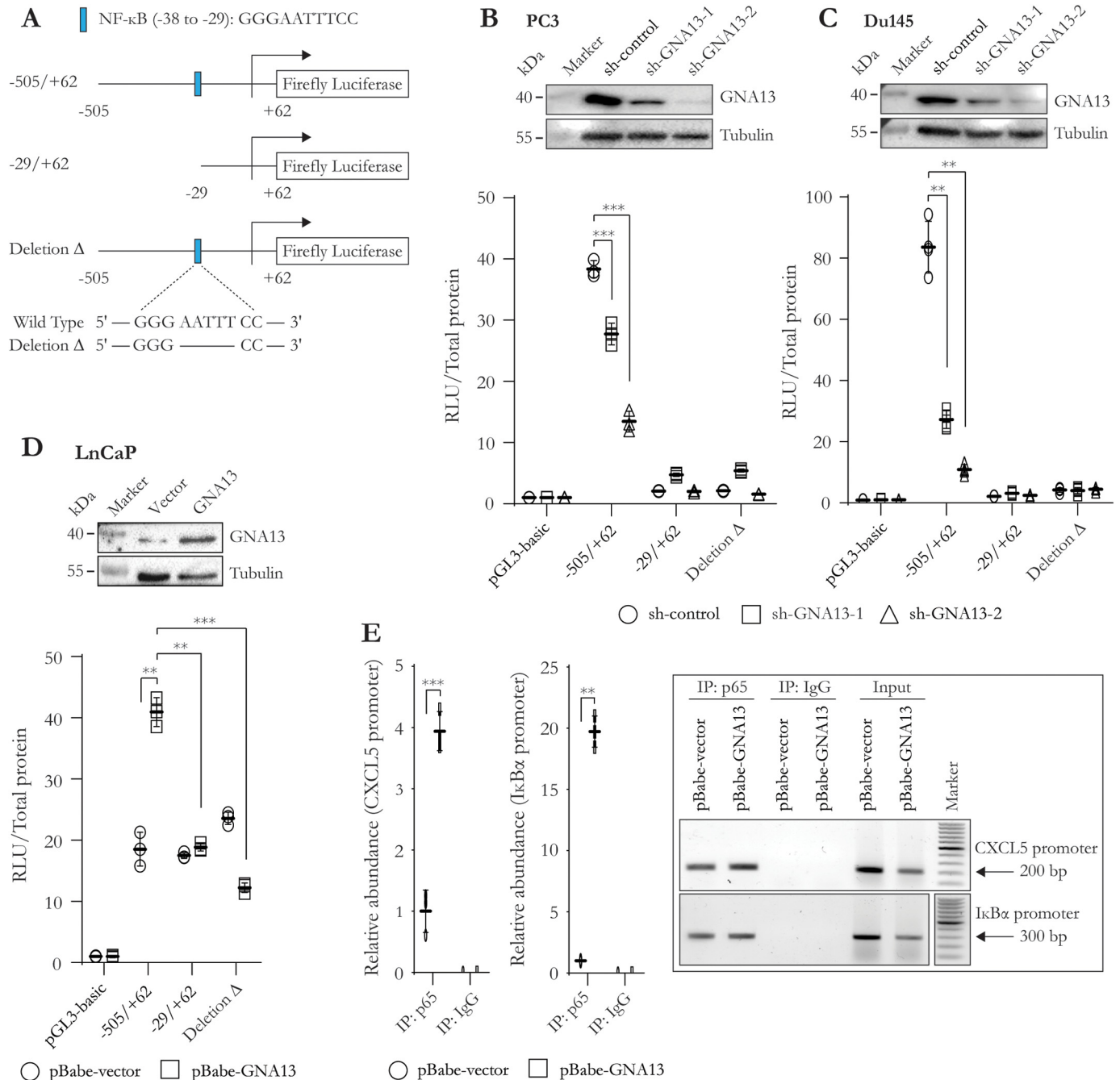


Figure 4. GNA13 induces CXCL5 expression through NF-κB. A, schematic diagram of the CXCL5 promoter reporter constructs with disrupted NF-κB-binding sites. The position of the identified NF-κB-binding site within the CXCL5 -505/+62 region is shown as the blue bar. The NF-κB-binding site was removed via truncation or deletion mutation as described under "Experimental procedures." B-D, importance of the NF-κB-binding site for GNA13-induced CXCL5 promoter activity. Shown is the effect of removing or mutating the NF-κB-binding site on GNA13-dependent promoter activity in PC3 (B), Du145 (C), and LnCaP (D) cells. For PC3 and Du145 cells, the data come from both control cells and those expressing sh-GNA13-1 or sh-GNA13-2 as indicated. For LnCaP cells, the data come from cells expressing pBabe-GNA13 compared with pBabe-vector. GNA13 expression for each of the cells is shown in immunoblots in B-D. E, GNA13 induces the binding of the p65 subunit of the NF-κB transcriptional factor complex to the CXCL5 promoter. Data shown represent the abundance of p65-bound CXCL5- and IκBα-gene promoter fragments recovered from the ChIP assays in LnCaP cells expressing pBabe-GNA13 relative to that of cells expressing pBabe-vector. ChIP-qPCR analysis was performed as described under "Experimental procedures," and the amplification of the immunoprecipitated chromatin was calculated as the fold-change relative to vector control cells using the $2^{-\Delta\Delta Ct}$ method. Immunoprecipitation with IgG was included as a negative control. Immunoprecipitated DNA was amplified by real-time PCR using primers specifically designed to amplify regions upstream and downstream of the NF-κB-binding site within the CXCL5 and IκBα gene promoters, producing a PCR product of 200 and 300 bp for CXCL5 and IκBα, respectively. DNA gel analysis of the amplified PCR products of qPCR is shown in E. p values are calculated from three independent biological repeats of the same experiment; results shown are a representative of those three. Plotted data are presented as mean ± S.D., and p values are denoted as follows: *, $p < 0.05$; **, $p < 0.01$; and ***, $p < 0.001$.

However, despite these studies emphasizing the importance of GNA13 in drug resistance and tumor progression, the molecular mechanisms that mediate the pronounced impact of

GNA13 on tumorigenesis and tumor progression are not well-understood. In this study, using prostate cancer cells as a model, we present evidence of one such mechanism: GNA13 acts

GNA13 induces CXCL5 expression in prostate cancers

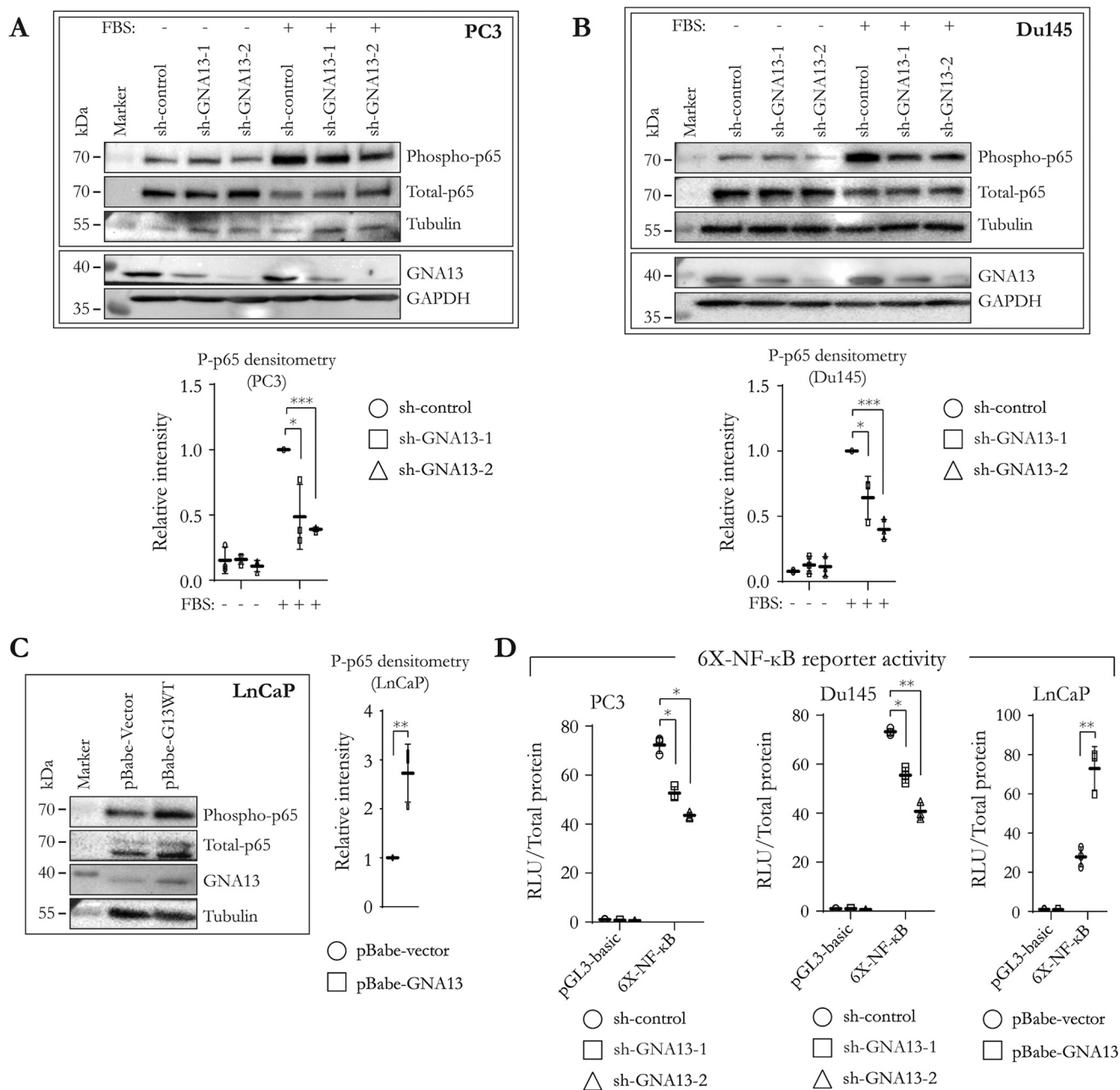


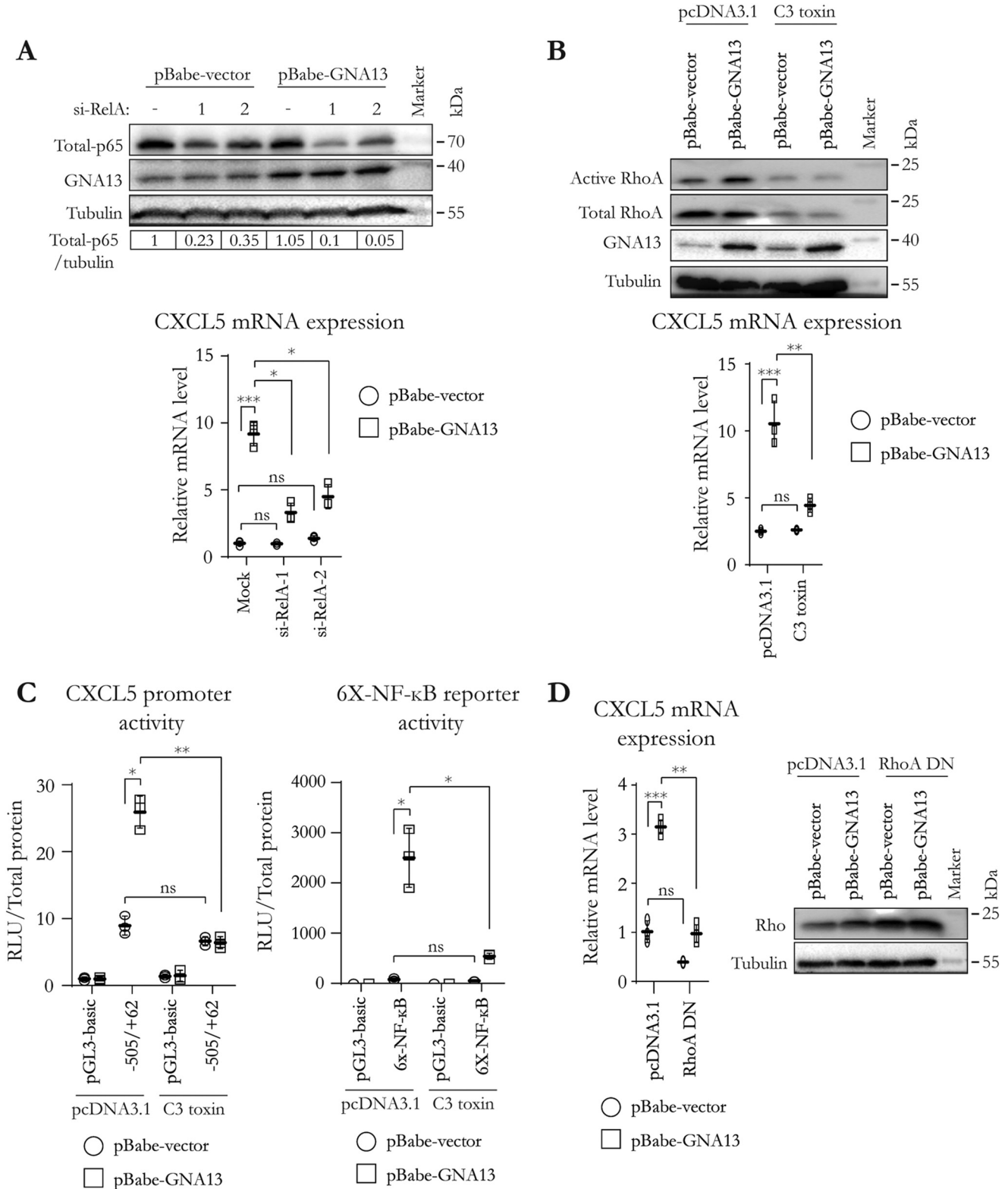
Figure 5. GNA13 levels impact NF-κB/p65 phosphorylation and transcriptional activity. *A* and *B*, knockdown of GNA13 suppresses phosphorylation of p65 in prostate cancer cells. Impact of knockdown of GNA13 in PC3 (*A*) and Du145 (*B*) cells on FBS-induced phosphorylation of p65, a major component of the NF-κB-signaling pathway. Shown is the immunoblot analysis of the effect of GNA13 knockdown (*sh-GNA13-1* or *sh-GNA13-2*, compared with *sh-control*) on NF-κB activation under serum-starvation and -stimulation conditions. Phosphorylated p65 (*phospho-p65*) was detected using a phospho-p65 antibody (Ser-536) whereas total p65 was probed with a p65-specific antibody; tubulin or glyceraldehyde-3-phosphate dehydrogenase was used as loading controls as indicated. To quantify p65 phosphorylation, individual band intensities were measured by Image Lab™ software, and the phosphorylated signal was divided by that of total protein followed by the loading control and further normalized to the serum-stimulated control cell line. Densitometry for p65 phosphorylation and statistical analysis is calculated from three biological replicates and represented as a *graph* below the immunoblots. *C*, enforced expression of GNA13 induces NF-κB activation in LnCaP cells. Shown is immunoblot analysis of the effect of GNA13 overexpression (pBabe-GNA13 versus pBabe-vector) on p65 phosphorylation under the serum-containing growth conditions. The *graph* represents quantification of phospho-p65 levels in GNA13-expressing cells compared with vector control. *D*, impact of GNA13 levels on NF-κB promoter activity in three prostate cancer cell lines. Shown is the activity of NF-κB-driven firefly luciferase expression from a reporter element consisting of six repeats of the NF-κB (6X-NF-κB) consensus sequence driving luciferase expression. The impact of knockdown of GNA13 (*sh-GNA13-1* or *sh-GNA13-2* as compared with *sh-control*) in PC3 (*left panel*) and Du145 (*middle panel*) on promoter reporter activity is shown, as well as the impact of overexpression of GNA13 in LnCaP cells (*right panel*, cells expressing pBabe-GNA13 compared with pBabe-vector). The RLU values were normalized to total protein and plotted as fold-change relative to the pGL3-basic vector control for each cell line. *p* values are calculated from three independent biological repeats of the same experiment; results shown are a representative of those three. Plotted data are presented as mean ± S.D., and *p* values are denoted as follows: *, *p* < 0.05; **, *p* < 0.01; and ***, *p* < 0.001.

GNA13 induces CXCL5 expression in prostate cancers

through Rho GTPases to drive an NF- κ B transcriptional program to induce CXCL5 expression in prostate cancer cells.

Several lines of evidence have provided a link between NF- κ B function and the expression of CXCL5 and also several other chemokines that modulate the tumor microenvironment (31). One such example is that dysregulation of NF- κ B can lead to

aberrant expression of CXCL5 in many diseases, including cancers (32, 33). In addition to impacting the immune microenvironment of a tumor, increased NF- κ B transcriptional activity has been implicated in inducing multiple hallmarks of solid tumors, including tumor initiation, cancer cell proliferation, resistance to apoptosis, epithelial–mesenchymal transi-



GNA13 induces CXCL5 expression in prostate cancers

tion, and metastasis (34). Given the pleiotropic role of NF- κ B in tumorigenesis and progression, it is not surprising that studies on elucidating the mechanisms that activate NF- κ B signaling in cancers have led to the identification of multiple cell-surface receptors, including receptors for tumor necrosis factor- α and interleukins as the major drivers of this pathway (34).

Recently, GPCRs, especially those that signal through G_q or G₁₂ proteins, have been reported to modulate NF- κ B signaling in cancers (35, 36). In this regard, a recent study reported evidence that GNA13 induces NF- κ B activation and chemokine expression in colorectal cancer (37). Interestingly, unlike prostate cancers, the GNA13–NF- κ B axis in colorectal cancer seems to drive a different set of chemokines, namely CXCL1, -2, and -4 but not CXCL5 (37). This is noteworthy because, despite being driven by largely similar mechanisms, the type of CXC-chemokines that are regulated by GNA13 appear to be dependent on the cell type examined. In addition, in this study we identified Rho GTPases as crucial intermediate players of the GNA13–NF- κ B–CXCL5-signaling cascade, presenting a more detailed mechanism of GNA13-dependent chemokine regulation in the context of prostate cancers. We also examined whether Rho-associated protein kinase (ROCK) is involved in the activation of GNA13-dependent CXCL5 expression, but interestingly, we did not see any impact of ROCK inhibition (Fig. S3).

Also noteworthy is a previous report showing that some GNA13-coupled GPCRs, including PAR1, LPAR, and S1PR, can induce proinflammatory signals via activating the RhoA–NF- κ B–signaling pathway (38). Interestingly, this study also elucidated a molecular mechanism for this effect by showing that GPCR activation induced phospholipase C_e, leading to sustained activity of diacylglycerol-regulated kinase and protein kinase D and ultimately leading the activation of NF- κ B (38). Similar mechanisms may be involved in GNA13-induced NF- κ B activation via RhoA in prostate cancer cells; this is currently under investigation. Elevated levels of GNA12, unlike GNA13, did not induce CXCL5 expression in prostate cancer cells. One possible explanation is the finding that GNA12 does not impact the activation of the crucial intermediary of the GNA13–NF- κ B signaling axis described here, Rho (Fig. S4) in prostate cancer cells. Although this finding is surprising, we have previously reported that the activation of Rho by G₁₂ proteins can occur in a cell type-specific manner (39, 40). The lack of RhoA activation by GNA12 is likely a property of prostate and possibly several other cancer cells.

It is also interesting to note that CXC-chemokines are important for both physiological and tumor-induced angiogenesis (32), where it has been reported that CXCL5 expression is up-regulated in metastatic prostate cancers and induces cell proliferation, migration, and metastasis through induction of angiogenesis (18). Noteworthy in this regard is that early studies in mice showed that knockout of GNA13 induces embryonic lethality due to a defective angiogenesis (41). In terms of tumor angiogenesis, two different studies have shown that GNA13 impacts tumor growth by inducing tumor angiogenesis either by inducing VEGFR-2 expression in endothelial cells (42) or by inducing pro-angiogenic CXCL1, -2, and -4 secretion by tumor cells (37). Interestingly, a gene set enrichment analysis of our RNA-Seq data showed a significant (p value = 0.00992) loss of pro-angiogenic genes upon silencing of GNA13 expression in prostate cancer cells (Fig. S5). Together with findings that both GNA13 and CXCL5 induce epithelial-to-mesenchymal transition, induction of cancer stem cell-like phenotype, drug resistance, and prostate cancer cell migration and metastasis (13, 16, 17, 21, 43), these data suggest that GNA13-induced tumorigenesis and progression might be mediated by its ability to induce expression of multiple pro-tumorigenic and pro-angiogenic chemokines in prostate cancers. Taken together, these data indicate that GNA13 induces a global NF- κ B transcriptional program that could contribute to tumor growth and progression in many different solid tumors.

In summary, this study presents a novel finding of interplay between GNA13 levels and CXCL5 expression in prostate cancer cells. Elucidation of the basic underlying mechanisms of this process in multiple prostate cancer cell lines revealed that GNA13, through Rho, can drive NF- κ B signaling and stimulate CXCL5 expression. Because both NF- κ B signaling and CXCL5 are known to induce tumor growth and progression by modulating the tumor microenvironment, it will be important now to study this process *in vivo*. Given the importance of NF- κ B and its transcriptional targets in tumor progression, developing novel therapeutic strategies targeting GNA13 could lead to enhanced therapeutic options for prostate cancer in the future.

Experimental procedures

Cell lines, transfection, and reagents

PC3, Du145, and LnCaP cells were purchased from the ATCC. PC3 and Du145 cells stably expressing sh-RNA against GNA13 (either sh-GNA13-1 or sh-GNA13-2) and cells

Figure 6. GNA13 control of CXCL5 expression requires NF- κ B and depends on Rho GTPases. *A*, knockdown of the p65 component of NF- κ B suppresses GNA13-induced CXCL5 expression. The *top panel* shows immunoblot analysis of total p65 levels in LnCaP vector control cells and those stably overexpressing GNA13 subjected to knockdown of p65 using two different si-RNAs (*si-RelA-1* and -2). Total p65 level was quantified by measuring individual band intensities using Image Lab™ software, and the protein signal was divided by that of the loading control and further normalized to the mock-transfected pBabe-vector cells. The *lower panel* shows the effect of p65 suppression on CXCL5 mRNA levels in LnCaP cells; mRNA expression was plotted as fold-change relative to the mock-transfected pBabe-vector cells. *B*, inhibition of Rho GTPase activity abrogates GNA13-induced CXCL5 expression. The *top panel* shows immunoblot analysis of the effect of C3 toxin treatment on RhoA activation status, where active Rho was isolated using a GST-Rhotekin pull-down assay. The *lower panel* shows the effect of C3 toxin treatment on CXCL5 mRNA levels, which are plotted as fold-change to pBabe-vector control cells. *C*, inhibition of Rho GTPase activity diminishes GNA13-dependent CXCL5- and NF- κ B–promoter reporter activities in LnCaP cells. The effect of C3 toxin treatment of control LnCaP cells (pBabe-vector) and those overexpressing GNA13 (pBabe-GNA13) on CXCL5-promoter (*left panel*) or 6X-NF- κ B reporter (*right panel*)-driven luciferase expression is shown. Data reflect the ratio of RLU of the reporters normalized to total protein amount and plotted as fold-change relative to the pBabe-vector control cells. *D*, expression of dominant-negative RhoA (*RhoA DN*) blocks GNA13-induced CXCL5 mRNA expression in LnCaP cells. The *left panel* shows the effect of dominant-negative RhoA (indicated as *RhoA-DN*) on GNA13-induced CXCL5 mRNA levels in LnCaP cells (pBabe-vector or pBabe-GNA13, respectively), plotted as fold-change to the pBabe-vector control cells. The *right panel* shows immunoblot analysis of Rho protein levels following the introduction of dominant-negative RhoA in the cells. p values are calculated from three independent biological repeats of the same experiment; results shown are a representative of those three. Plotted data are presented as mean \pm S.D., and p values are denoted as follows: *, $p < 0.05$; **, $p < 0.01$; and ***, $p < 0.001$ or *ns* for not significant.

expressing the control sh-RNA (sh-RNA-control) were used as GNA13 knockdown cell models of human prostate cancer. A GNA13 overexpression cell model was also created consisting of LnCaP cells stably expressing pBabe-vector (a gift from Dr. Mathijs Voorhoeve) or pBabe-GNA13. The cloning strategy of these constructs has been described previously (16). For rescue experiments, a GNA13 cDNA construct that is resistant to the sh-RNA targeting GNA13 was cloned in a tetracycline-controlled inducible system (Tet-On® 3G Inducible Expression Systems, Takara Bio USA Inc.). Cells were cultured in RPMI 1640 medium (catalog no. 22400-089, Gibco, Thermo Fisher Scientific) supplemented with 10% FBS (catalog no. 10500064, Invitrogen), 1% penicillin/streptomycin (catalog no. 15140-122, Gibco, Thermo Fisher Scientific), and 1% antibiotic/antimycotic (catalog no. 15240-062, Gibco, Thermo Fisher Scientific). GNA13 knockdown cell lines were maintained in the presence of 10 µg/ml blasticidin S hydrochloride (catalog no. 3513-03-9, Sigma). LnCaP GNA13 overexpression cells were grown with 5 µg/ml puromycin dihydrochloride (catalog no. P8833, Sigma). Tetracycline-inducible PC3 cells were grown in 10 µg/ml blasticidin, along with 50 µg/ml G418 (catalog no. 108321-42-2, Gold-Bio) and 0.5 µg/ml of puromycin. All cells were used to a maximum of 10 passages for experiments and were maintained at 37 °C with 5% CO₂. Transfection of plasmids or si-RNA was performed using either JETPRIME transfection reagent (catalog no. 114-07, Polyplus Transfection, France) or Lipofectamine™ 2000 (catalog no. 11668019, Invitrogen), according to the manufacturer's protocol. Culture media were replaced 6 h post-transfection without selection markers. The details of all commercial si-RNAs used are listed in Table S2. ROCK inhibitor Y-27632 was purchased from Sigma (catalog no. Y0503); AR-13324 (netarsudil) was a kind gift from Dr. David Epstein (Duke-NUS Medical School).

Total RNA extraction, cDNA synthesis, and quantitative real-time PCR analysis

Total RNA was extracted from cells at 80% confluency using the RNeasy Mini kit (catalog no. 74106, Qiagen, Germany) according to the manufacturer's protocol. RNA (1 µg) was reverse-transcribed using the iSCRIPT cDNA synthesis kit (catalog no. 170-8891, Bio-Rad), according to the manufacturer's protocol, and the resultant cDNA was diluted 5-fold in nuclease-free water to a final concentration of 10 ng/µl. RNA expression was analyzed by real-time PCR using iQ™ SYBR® Green Supermix (catalog no. 1708880, Bio-Rad) according to the manufacturer's protocol. Briefly, each real-time PCR is made up of 1× iQ™ SYBR® Green Supermix, 0.5 µM of each gene-specific primer, 25 ng of cDNA, and nuclease-free water to a reaction volume of 10 µl. HPRT was included as a normalizing control gene. Relative mRNA expression of a specific gene was determined using the standard 2^{-ΔΔC_t} method (39, 45). Sequences of PCR primers used are listed in Table S3.

Protein extraction and immunoblot analysis

For whole-cell lysate preparation, cells were first washed with ice-cold PBS and lysed with Tris lysis buffer (50 mM Tris buffer, pH 6.8, 150 mM NaCl, 1.5 mM MgCl₂, 1 mM EDTA, 1 mM EGTA, 1% Triton X-100, and 6% glycerol) supplemented with

protease (Complete ULTRA Tablets, catalog no. 05892970001, Roche Applied Science, Germany) and phosphatase inhibitors (PhosSTOP ULTRA Tablets, catalog no. 04906837001, Roche Applied Science, Germany). Protein was quantified using the BCA protein quantification kit (catalog no. 23223, Thermo Fisher Scientific), diluted in Tris lysis buffer and 2× Laemmli sample buffer (catalog no. 161-0737, Bio-Rad) containing β-mercaptoethanol, and denatured at 95 °C for 10 min. For immunoblot analysis, briefly, equal amounts of protein were separated on SDS-polyacrylamide gels and blotted onto polyvinylidene difluoride membranes using wet transfer. Membranes were then blocked with 5% nonfat dry milk at room temperature and probed with specific antibodies targeting proteins of interest overnight at 4 °C. Immunoblots were washed with 1× TBS-T (Tris-buffered saline with 0.1% Tween 20), incubated with respective secondary antibodies, washed again, and then visualized by chemiluminescence (Pierce® ECL Western blotting substrate, catalog no. 32106, or SuperSignal™ West Femto Maximum Sensitivity Substrate, catalog no. 34096, Thermo Fisher Scientific). The details of all antibodies used are listed in Table S4.

ELISA

Assays were conducted using supernatant collected from cultured cells. 250,000 cells were first seeded into 6-well plates and cultured for 48 h. Cell culture supernatants were then collected, briefly centrifuged at 1,500 rpm to remove cell debris, and assayed for CXCL5 using human CXCL5/ENA-78 Quantikine ELISA kit (catalog no. DX000, R&D Systems) according to the manufacturer's protocol. Briefly, 50 µl of conditioned media was loaded into each well (96-well format) that had been pre-coated with mAb directed against human CXCL5. The assay plate was then incubated for 2 h at room temperature with rotation, washed to remove unbound proteins, incubated with enzyme-linked polyclonal secondary antibody, washed again, and finally incubated with substrate solution for 30 min at room temperature in the dark before the colorimetric reaction was terminated. Absorbance was measured at 450 and 540 nm. Results were analyzed by correcting absorbance reading at 450 nm from that at 540 nm, and the values were plotted as fold-change to the relevant controls.

GST-rhotekin-active Rho pulldown assay

Intracellularly-active Rho (Rho-GTP) was isolated using the active Rho pulldown and detection kit (catalog no. 16116, Thermo Fisher Scientific), according to the manufacturer's protocol. Briefly, cells (LnCaP, 2.5 × 10⁶; Du145, 8 × 10⁵) were seeded into 10-cm dishes, treated, and cultured for appropriate durations. Cells were then washed with ice-cold PBS and lysed with Rho lysis buffer supplemented with protease and phosphatase inhibitors. Lysates were centrifuged at 16,000 × g for removal of cell debris, from which a fraction of protein lysate was stored as total input while the remaining was incubated with GST-rhotekin-RBD-coupled GSH-Sepharose resin beads at 4 °C for 1.5 h with rotation. Active Rho protein-bound beads were then washed and eluted twice in 2× Laemmli buffer containing β-mercaptoethanol to a final volume of 50 µl. The eluted samples were denatured at 95 °C for 5 min, resolved on a

GNA13 induces CXCL5 expression in prostate cancers

12% SDS-polyacrylamide gel, and quantified using immunoblotting. For Du145 cells, cells were serum-starved for 6 h and stimulated with 10% serum-containing media at 70% confluency for the appropriate duration prior to extraction.

CXCL5 promoter cloning

Genomic DNA was extracted from PC3 WT cells using DNeasy Blood and Tissue kit (catalog no. 69504, Qiagen, Germany) and was used as a template to amplify the promoter region of human CXCL5. PCR was performed using iPROOF high-fidelity PCR kit (catalog no. 072–5301, Bio-Rad), according to the manufacturer's protocol. PCR primers were designed with MluI and BglII restriction sites; sequences of the PCR primers used are listed in Table S5. The PCR products were purified using NucleoSpin® gel and PCR clean-up kit (740609.50, Macherey-Nagel, Germany) and cloned into pGL3-basic vector at the MluI and BglII restriction sites (MluI, catalog no. R3198L, and BglII, catalog no. R0144S, New England Biolabs, London, UK) upstream of the promoter-less firefly luciferase gene. To generate the CXCL5 promoter deletion mutant construct, five nucleotides (AATTT) within the NF- κ B-binding region were deleted using site-directed mutagenesis with iPROOF high-fidelity PCR kit. The linear plasmid harboring the deletion was treated with T4 polynucleotide kinase (catalog no. M0201S, New England Biolabs, London, UK), re-circularized, transformed into bacteria, and amplified as per the previously established protocols of the lab (39). 6X-NF- κ B-luciferase reporter contains six repeats of the NF- κ B-binding consensus sequence driving the luciferase gene and is a gift from Prof. Doris Mayer, Germany, and further details are described previously (46).

Luciferase reporter assay

For luciferase reporter assays, 60,000 cells were seeded into 24-well plates in quadruplicate and allowed to settle, whereupon 500 ng of pGL3-basic vector, the respective CXCL5 promoter DNA constructs, or the 6X-NF- κ B-luciferase reporter was transfected into cells. Luciferase reporter assays were conducted 48 h post-transfection. Briefly, cell culture media were aspirated, and cells were lysed with passive lysis buffer (catalog no. E194A, Promega) followed by incubation at room temperature for 10 min with rocking. Cell lysates were then collected and centrifuged at $2000 \times g$ for 5 min to remove cell debris. Firefly luciferase assay substrate (catalog no. E1501, Promega) was added and incubated for 10 min at room temperature, and luminescence was measured as a readout for promoter activity. The remaining lysates were used for total protein quantification using BCA protein quantification kit. The activity of each promoter-reporter construct was determined as relative light units by dividing the firefly luciferase luminescence value with the optical density obtained from total protein quantification and then further normalized to the promoter-less (pGL3-Basic) control.

ChIP

To assess binding of NF- κ B to the CXCL5 promoter element, 2×10^7 cells were collected in a tube, fixed with freshly prepared formaldehyde (catalog no. F8775, Sigma) to a final concentration of 1% for 10 min at room temperature, and

quenched with freshly made 2 M glycine to a final concentration of 0.4 M. Cells were then centrifuged at $300 \times g$ for 5 min, washed twice with PBS, and then lysed with cell lysis buffer (10 mM HEPES, 10 mM EDTA, 0.5 mM EGTA, 0.25% Triton X-100) supplemented with protease inhibitors and 0.1 mM PMSF. Nuclei were obtained by centrifugation of the cell lysate at $500 \times g$ for 5 min followed by lysis with nuclei lysis buffer (10 mM HEPES, 200 mM NaCl, 1 mM EDTA, 0.5 mM EGTA, 0.01% Triton X-100) supplemented with protease inhibitors and 0.1 mM PMSF. The nuclear fraction was isolated and resuspended in ChIP buffer (25 mM Tris-HCl, 150 mM NaCl, 2 mM EDTA, 1% Triton X-100, 0.25% SDS) supplemented with protease inhibitors and 0.1 mM PMSF. Chromatin samples were sonicated to obtain DNA fragments of 300–600 bp in length followed by 3-fold dilution in $3 \times$ ChIP buffer (25 mM Tris-HCl, 150 mM NaCl, 2 mM EDTA, 1% Triton X-100, 7.5% glycerol) that is supplemented with protease inhibitors and 0.1 mM PMSF. For immunoprecipitation, Dynabeads™ protein G magnetic beads (catalog no. 10004D, Invitrogen) were first preincubated with 0.5% BSA and 4 μ g of IgG control antibody or NF- κ B p65 antibody (catalog no. 17-10060, Merck) for 2 h at 4 °C with rotation followed by incubation with sheared chromatin overnight at 4 °C with rotation. Beads were then washed with low-salt wash buffer (20 mM Tris-HCl, 150 mM NaCl, 2 mM EDTA, 1% Triton X-100, and 0.1% SDS), high-salt wash buffer (20 mM Tris-HCl, 500 mM NaCl, 2 mM EDTA, 1% Triton X-100, and 0.1% SDS), LiCl buffer (10 mM Tris-HCl, 250 mM LiCl, 1 mM EDTA, 0.5% Nonidet P-40, 0.5% sodium deoxycholate), and TE buffer (10 mM Tris-HCl, 50 mM NaCl, 1 mM EDTA). The chromatin was eluted in elution buffer (100 mM sodium bicarbonate and 1% SDS) at room temperature for 15 min with agitation and reverse cross-linked with 50 mg of proteinase K overnight at 65 °C with shaking. Finally, the immunoprecipitated chromatin was purified using Agencourt AMPure XP PCR purification kit (catalog no. A63881, Beckman Coulter), according to the manufacturer's protocol, and analyzed by real-time PCR.

RNA-Seq and analysis

PC3 cells (1×10^6) harboring the control sh-RNA or two different sh-RNAs directed against GNA13 were seeded in 10-cm dishes and cultured for 48 h until the cells reached 80% confluency. Total RNA was extracted (RNeasy kit, Qiagen), and sequencing libraries were generated using an Illumina TruSeq mRNA library kit according to the manufacturer's instructions. Paired-end sequencing of 2×100 bp was conducted via Illumina HiSeq 4000 according to the manufacturer's instructions (Illumina). The RNA-Seq was performed by Theragen (Republic of Korea). The raw read files were checked for sequencing quality via FastQC program (<https://www.bioinformatics.babraham.ac.uk/projects/fastqc/>)⁴ and subsequently mapped to the human reference genome (GRCh37) via the STAR version 2.1.3 aligner (47). Mapped reads were quantified for gene and transcript abundance estimation via Cufflinks version 2.2.1 (9) and further analyzed for differential gene expression via Cuffdiff version 2.2.1 (44).

⁴ Please note that the JBC is not responsible for the long-term archiving and maintenance of this site or any other third party hosted site.

Statistical analysis

All experiments were performed at least three times, and each with three or four technical replicates, where appropriate. A representative experiment is shown in most figures, and the *p* values presented are calculated from pooled values from three independent biological replicates of these experiments using analysis of variance ($n = 9$ or 12). For Western blotting quantification graphs, Student's *t* test was used to calculate the *p* values using values from three independent experiments ($n = 3$). A *p* value of <0.05 was considered significant.

Author contributions—W. K. L., S. A. K. R., and P. J. C. conceptualization; W. K. L., S. A. K. R., and P. J. C. formal analysis; W. K. L., S. A. K. R., and P. J. C. validation; W. K. L., S. A. K. R., and P. J. C. investigation; W. K. L., S. G., S. A. K. R., and P. J. C. visualization; W. K. L., D. R., S. A. K. R., and P. J. C. methodology; W. K. L., M. W., S. A. K. R., and P. J. C. writing—original draft; W. K. L., S. A. K. R., and P. J. C. project administration; W. K. L., M. W., S. A. K. R., and P. J. C. writing—review and editing; X. C., S. G., and S. A. K. R. data curation; X. C. and S. G. software; S. G., S. A. K. R., and P. J. C. supervision; S. A. K. R. and P. J. C. funding acquisition; P. J. C. resources; X. C. and S. G. RNA sequencing analysis.

References

- Siegel, R. L., Miller, K. D., and Jemal, A. (2019) Cancer statistics, 2019. *CA Cancer J. Clin.* **69**, 7–34 [CrossRef Medline](#)
- Bray, F., Ferlay, J., Soerjomataram, I., Siegel, R. L., Torre, L. A., and Jemal, A. (2018) Global cancer statistics 2018: GLOBOCAN estimates of incidence and mortality worldwide for 36 cancers in 185 countries. *CA Cancer J. Clin.* **68**, 394–424 [CrossRef Medline](#)
- Litwin, M. S., and Tan, H. J. (2017) The diagnosis and treatment of prostate cancer: a review. *JAMA* **317**, 2532–2542 [CrossRef Medline](#)
- Daaka, Y. (2004) G proteins in cancer: the prostate cancer paradigm. *Sci. STKE* 2004, re2 [CrossRef Medline](#)
- Rohrer, D. K., and Kobilka, B. K. (1998) G protein-coupled receptors: functional and mechanistic insights through altered gene expression. *Physiol. Rev.* **78**, 35–52 [CrossRef Medline](#)
- Dorsam, R. T., and Gutkind, J. S. (2007) G-protein-coupled receptors and cancer. *Nat. Rev. Cancer* **7**, 79–94 [CrossRef Medline](#)
- Rosenbaum, D. M., Rasmussen, S. G., and Kobilka, B. K. (2009) The structure and function of G-protein-coupled receptors. *Nature* **459**, 356–363 [CrossRef Medline](#)
- Kelly, P., Casey, P. J., and Meigs, T. E. (2007) Biologic functions of the G12 subfamily of heterotrimeric G proteins: growth, migration, and metastasis. *Biochemistry* **46**, 6677–6687 [CrossRef Medline](#)
- Trapnell, C., Williams, B. A., Pertea, G., Mortazavi, A., Kwan, G., van Baren, M. J., Salzberg, S. L., Wold, B. J., and Pachter, L. (2010) Transcript assembly and quantification by RNA-Seq reveals unannotated transcripts and isoform switching during cell differentiation. *Nat. Biotechnol.* **28**, 511–515 [CrossRef Medline](#)
- Offermanns, S. (2010) *In vivo* functions of heterotrimeric G-proteins: studies in G α -deficient mice. *Oncogene* **20**, 1635–1642 [CrossRef Medline](#)
- Kelly, P., Moeller, B. J., Juneja, J., Booden, M. A., Der, C. J., Daaka, Y., Dewhirst, M. W., Fields, T. A., and Casey, P. J. (2006) The G12 family of heterotrimeric G proteins promotes breast cancer invasion and metastasis. *Proc. Natl. Acad. Sci. U.S.A.* **103**, 8173–8178 [CrossRef Medline](#)
- Kelly, P., Stemmler, L. N., Madden, J. F., Fields, T. A., Daaka, Y., and Casey, P. J. (2006) A role for the G12 family of heterotrimeric G proteins in prostate cancer invasion. *J. Biol. Chem.* **281**, 26483–26490 [CrossRef Medline](#)
- Rasheed, S. A. K., Leong, H. S., Lakshmanan, M., Raju, A., Dadlani, D., Chong, F. T., Shannon, N. B., Rajarethinam, R., Skanthakumar, T., Tan, E. Y., Hwang, J. S. G., Lim, K. H., Tan, D. S., Ceppi, P., Wang, M., et al. (2018) GNA13 expression promotes drug resistance and tumor-initiating phenotypes in squamous cell cancers. *Oncogene* **37**, 1340–1353 [CrossRef Medline](#)
- Gan, C. P., Patel, V., Mikelis, C. M., Zain, R. B., Molinolo, A. A., Abraham, M. T., Teo, S.-H., Abdul Rahman, Z. A., Gutkind, J. S., and Cheong, S. C. (2014) Heterotrimeric G-protein α -12 (G α 12) subunit promotes oral cancer metastasis. *Oncotarget* **5**, 9626–9640 [CrossRef Medline](#)
- Zhang, J.-X., Yun, M., Xu, Y., Chen, J.-W., Weng, H.-W., Zheng, Z.-S., Chen, C., Xie, D., and Ye, S. (2016) GNA13 as a prognostic factor and mediator of gastric cancer progression. *Oncotarget* **7**, 4414–4427 [CrossRef Medline](#)
- Rasheed, S. A., Teo, C. R., Beillard, E. J., Voorhoeve, P. M., and Casey, P. J. (2013) MicroRNA-182 and microRNA-200a control G-protein subunit α -13 (GNA13) expression and cell invasion synergistically in prostate cancer cells. *J. Biol. Chem.* **288**, 7986–7995 [CrossRef Medline](#)
- Rasheed, S. A., Teo, C. R., Beillard, E. J., Voorhoeve, P. M., Zhou, W., Ghosh, S., and Casey, P. J. (2015) MicroRNA-31 controls G protein α -13 (GNA13) expression and cell invasion in breast cancer cells. *Mol. Cancer* **14**, 67 [CrossRef Medline](#)
- Begley, L. A., Kasina, S., Mehra, R., Adsule, S., Admon, A. J., Lonigro, R. J., Chinnaiyan, A. M., and Macoska, J. A. (2008) CXCL5 promotes prostate cancer progression. *Neoplasia* **10**, 244–254 [CrossRef Medline](#)
- Zhou, S.-L., Dai, Z., Zhou, Z.-J., Chen, Q., Wang, Z., Xiao, Y.-S., Hu, Z.-Q., Huang, X.-Y., Yang, G.-H., Shi, Y.-H., Qiu, S.-J., Fan, J., and Zhou, J. (2014) CXCL5 contributes to tumor metastasis and recurrence of intrahepatic cholangiocarcinoma by recruiting infiltrative intratumoral neutrophils. *Carcinogenesis* **35**, 597–605 [CrossRef Medline](#)
- Kawamura, M., Toiyama, Y., Tanaka, K., Saigusa, S., Okugawa, Y., Hiro, J., Uchida, K., Mohri, Y., Inoue, Y., and Kusunoki, M. (2012) CXCL5, a promoter of cell proliferation, migration and invasion, is a novel serum prognostic marker in patients with colorectal cancer. *Eur. J. Cancer* **48**, 2244–2251 [CrossRef Medline](#)
- Kuo, P.-L., Chen, Y.-H., Chen, T.-C., Shen, K.-H., and Hsu, Y.-L. (2011) CXCL5/ENA78 increased cell migration and epithelial-to-mesenchymal transition of hormone-independent prostate cancer by early growth response-1/snail signaling pathway. *J. Cell. Physiol.* **226**, 1224–1231 [CrossRef Medline](#)
- O'Hayre, M., Degese, M. S., and Gutkind, J. S. (2014) Novel insights into G protein and G protein-coupled receptor signaling in cancer. *Curr. Opin. Cell Biol.* **27**, 126–135 [CrossRef Medline](#)
- Dhanasekaran, D. N. (2006) Transducing the signals: a G protein takes a new identity. *Sci. STKE* 2006, pe31 [CrossRef Medline](#)
- Suzuki, N., Hajicek, N., and Kozasa, T. (2009) Regulation and physiological functions of G12/13-mediated signaling pathways. *NeuroSignals* **17**, 55–70 [CrossRef Medline](#)
- Castellone, M. D., Laukkanen, M. O., Teramoto, H., Bellelli, R., Ali, G., Fontanini, G., Santoro, M., and Gutkind, J. S. (2015) Cross-talk between the bombesin neuropeptide receptor and Sonic hedgehog pathways in small cell lung carcinoma. *Oncogene* **34**, 1679–1687 [CrossRef Medline](#)
- Haug, G., Barth, H., and Aktories, K. (2006) Purification and activity of the Rho ADP-ribosylating binary C2/C3 toxin. *Methods Enzymol.* **406**, 117–127 [CrossRef Medline](#)
- Bian, D., Mahanivong, C., Yu, J., Frisch, S. M., Pan, Z. K., Ye, R. D., and Huang, S. (2006) The G12/13-RhoA signaling pathway contributes to efficient lysophosphatidic acid-stimulated cell migration. *Oncogene* **25**, 2234–2244 [CrossRef Medline](#)
- Yu, W., Beaudry, S., Negoro, H., Boucher, I., Tran, M., Kong, T., and Denker, B. M. (2012) H₂O₂ activates G protein, 12 to disrupt the junctional complex and enhance ischemia reperfusion injury. *Proc. Natl. Acad. Sci. U.S.A.* **109**, 6680–6685 [CrossRef Medline](#)
- Bhattacharyya, R., Banerjee, J., Khalili, K., and Wedegaertner, P. B. (2009) Differences in G α 12- and G α 13-mediated plasma membrane recruitment of p115-RhoGEF. *Cell. Signal.* **21**, 996–1006 [CrossRef Medline](#)
- Radhika, V., and Dhanasekaran, N. (2001) Transforming G proteins. *Oncogene* **20**, 1607–1614 [CrossRef Medline](#)
- Mantovani, A. (2010) Molecular pathways linking inflammation and cancer. *Curr. Mol. Med.* **10**, 369–373 [CrossRef Medline](#)

GNA13 induces CXCL5 expression in prostate cancers

32. Vandercappellen, J., Van Damme, J., and Struyf, S. (2008) The role of CXC-chemokines and their receptors in cancer. *Cancer Lett.* **267**, 226–244 [CrossRef Medline](#)
33. Mantovani, A., Savino, B., Locati, M., Zammataro, L., Allavena, P., and Bonecchi, R. (2010) The chemokine system in cancer biology and therapy. *Cytokine Growth Factor Rev.* **21**, 27–39 [CrossRef Medline](#)
34. Sen, R., and Baltimore, D. (2013) The complexity of NF- κ B signaling in inflammation and cancer. *Mol. Cancer* **12**, 1–15
35. Peeters, M. C., Fokkelman, M., Boogaard, B., Egerod, K. L., van de Water, B., IJzerman, A. P., and Schwartz, T. W. (2015) The adhesion G protein-coupled receptor G2 (ADGRG2/GPR64) constitutively activates SRE and NF κ B and is involved in cell adhesion and migration. *Cell. Signal.* **27**, 2579–2588 [CrossRef Medline](#)
36. Fraser, C. C. (2008) G protein-coupled receptor connectivity to NF- κ B in inflammation and cancer. *Int. Rev. Immunol.* **27**, 320–350 [CrossRef Medline](#)
37. Zhang, Z., Tan, X., Luo, J., Cui, B., Lei, S., Si, Z., Shen, L., and Yao, H. (2018) GNA13 promotes tumor growth and angiogenesis by upregulating CXC-chemokines via the NF- κ B signaling pathway in colorectal cancer cells. *Cancer Med.* **7**, 5611–5620 [CrossRef Medline](#)
38. Dusaban, S. S., Purcell, N. H., Rockenstein, E., Masliah, E., Cho, M. K., Smrcka, A. V., and Brown, J. H. (2013) Phospholipase C ϵ links G protein-coupled receptor activation to inflammatory astrocytic responses. *Proc. Natl. Acad. Sci. U.S.A.* **110**, 3609–3614 [CrossRef Medline](#)
39. Teo, C. R., Casey, P. J., and Rasheed, S. A. (2016) The GNA13-RhoA signaling axis suppresses expression of tumor protective kallikreins. *Cell. Signal.* **28**, 1479–1488 [CrossRef Medline](#)
40. Gohla, A., Harhammer, R., and Schultz, G. (1998) The G-protein G13 but not G12 mediates signaling from lysophosphatidic acid receptor via epidermal growth factor receptor to Rho. *J. Biol. Chem.* **273**, 4653–4659 [CrossRef Medline](#)
41. Offermanns, S. (2001) *In vivo* functions of heterotrimeric G-proteins: studies in G α -deficient mice. *Oncogene* **20**, 1635–1642 [CrossRef Medline](#)
42. Sivaraj, K. K., Takefuji, M., Schmidt, I., Adams, R. H., Offermanns, S., and Wettschureck, N. (2013) G13 controls angiogenesis through regulation of VEGFR-2 expression. *Dev. Cell* **25**, 427–434 [CrossRef Medline](#)
43. Liu, W., Li, H., Wang, Y., Zhao, X., Guo, Y., Jin, J., and Chi, R. (2017) MiR-30b-5p functions as a tumor suppressor in cell proliferation, metastasis and epithelial-to-mesenchymal transition by targeting G-protein subunit α -13 in renal cell carcinoma. *Gene* **626**, 275–281 [CrossRef Medline](#)
44. Trapnell, C., Hendrickson, D. G., Sauvageau, M., Goff, L., Rinn, J. L., and Pachter, L. (2013) Differential analysis of gene regulation at transcript resolution with RNA-seq. *Nat. Biotechnol.* **31**, 46–53 [CrossRef Medline](#)
45. Livak, K. J., and Schmittgen, T. D. (2001) Analysis of relative gene expression data using real-time quantitative PCR and the $2^{-\Delta\Delta CT}$ method. *Methods* **25**, 402–408 [CrossRef Medline](#)
46. Rasheed, S. A., Efferth, T., Asangani, I. A., and Allgayer, H. (2010) First evidence that the antimalarial drug artesunate inhibits invasion and *in vivo* metastasis in lung cancer by targeting essential extracellular proteases. *Int. J. Cancer* **127**, 1475–1485 [CrossRef Medline](#)
47. Dobin, A., Davis, C. A., Schlesinger, F., Drenkow, J., Zaleski, C., Jha, S., Batut, P., Chaisson, M., and Gingeras, T. R. (2013) STAR: ultrafast universal RNA-seq aligner. *Bioinformatics* **29**, 15–21 [CrossRef Medline](#)